Anomalous weak ferromagnetism in the magnetically frustrated system $R_{1-x}Y_xB_4$ (R=Tb and Dy)

B. Y. Kang,[1] J. Y. Kim,[2] H. Y. Choi,[3] and B. K. Cho[1,*]

[1]*School of Materials Science and Engineering, Gwangju Institute of Science and Technology, Gwangju 500-712, Korea*

[2]*Advanced Metallic Materials Research Department, Research Institute of Industrial Science and Technology, Pohang 790-330, Korea*

[3]*Department of Physics and Institute for Basic Science Research, Sungkyunkwan University, Suwon 400-746, Korea*

(Received 18 July 2014; revised manuscript received 3 October 2014; published 15 January 2015)

The magnetic properties of $R_{1-x}Y_xB_4$ (R = Tb and Dy) single crystals were investigated. As the concentration of Y increased, the antiferromagnetic transition temperature was observed to systematically decrease, and an exotic weak ferromagnetic transition was also observed at the antiferromagnetic transition temperature. The weak ferromagnetism occurred in the magnetic easy plane, (001) for $Tb_{1-x}Y_xB_4$, and along the magnetic easy axis, [001] for $Dy_{1-x}Y_xB_4$. For $Tb_{1-x}Y_xB_4$, the saturated ferromagnetic signal at $T = 2$ K was also anisotropic, even in the (001) plane; that is, there was a local maximum along the principal axis and a local minimum along the [110] axis (equivalent to those along Tb dimers), where the parent compound, TbB_4, was characterized as a magnetically frustrated dimer in a Shastry-Sutherland lattice. In addition, the saturated signal exhibited a strong dependence on the Y concentration, i.e., the signal reached a maximum at $x \simeq 0.35$, indicating that the emergence of the weak ferromagnetism is not due to an individual atomic effect but rather to a collective correlation effect. This is an experimental observation of the development of weak ferromagnetism in a magnetically frustrated system induced by replacing a magnetic element with a nonmagnetic element.

DOI: 10.1103/PhysRevB.91.024414 PACS number(s): 75.30.Cr, 75.50.Cc

I. INTRODUCTION

Geometrically frustrated magnetic systems have received considerable attention over the past few decades in condensed-matter physics [1–4]. In general, the combination of magnetism, either antiferromagnetism or ferromagnetism, with a certain crystal symmetry leads to magnetic frustration, which cannot simultaneously satisfy the magnetic long-range interactions between near-neighbor spins on the lattices. When the frustration is strong, the system exhibits a rich phase diagram, such as a lack of long-range magnetic ordering at low temperature, noncollinear ordering, novel critical exponents, and spin liquids. As a representative example, the pyrochlore $R_2Ti_2O_7$ (R = Tb, Ho, Tm) was intensively studied. $Tb_2Ti_2O_7$ was observed to be paramagnetic at low temperatures; despite the onset of antiferromagnetic short-range order at ∼50 K [2], $Ho_2Ti_2O_7$ formed a spin-ice state due to frustration from ferromagnetic exchange and strong anisotropy [1,3]. The frustrations in $ZnCr_2O_4$ were observed to involve spin clusters (not individual spins) [4], which provided theoretical models for various physical properties of geometrically frustrated magnets. Another interesting frustration was observed in the two-dimensional Heisenberg spin system $SrCu_2(BO_3)_2$ [5], in which the magnetic system is topologically equivalent to the Shastry-Sutherland lattice [6]. $SrCu_2(BO_3)_2$ was identified to have the exact dimer ground state in a Shastry-Sutherland lattice and to have antiferromagnetic interaction strength near the quantum phase transition from the dimer state to the antiferromagnetically ordered state [7]. Other interesting new physical ground states derived from frustrated magnetic interactions include spin-charge separation [8], charge ordering [9], the suppression of long-range ordering [10], a change in the spin dynamics [11], and the emergence of ferroelectricity [12]. In addition, doped Shastry-Sutherland lattice systems have been hypothesized to potentially exhibit superconductivity [13–15].

RB_4 (R = rare-earth elements) compounds belong to a geometrically frustrated magnetic system. The network of rare-earth ions, which have the same z position ($z = 0$) at the $4g$ sites of $P4/mbm$, forms the Shastry-Sutherland lattice. Although the crystallographic structure and physical properties are very similar, RB_4 compounds exhibit various interesting magnetic ground states depending on the rare-earth elements. These compounds exhibit an antiferromagnetic ordering at a low temperature (except PrB_4) with two types of easy axes: the easy axis of RB_4 (R = Nd, Eu, Gd, and Tb) is parallel to the (001) plane, and the easy axis of RB_4 (R = Dy, Ho, Er, Tm, and Yb) is perpendicular to the (001) plane [16,17]. In addition, RB_4 (R = Tb, Dy, and Ho) exhibited a second transition below the antiferromagnetic phase transition. The origin of the second transition was hypothesized to be a quadrupolar orbital fluctuation. The proportionality of the order parameters of the quadrupolar order and a strain in DyB_4 was the first experimental observation of the coupling between the two order parameters [18]. Quadrupolar or higher-rank multipolar ordered states were also suggested in NdB_4 [19]. The Ising-spin system ErB_4 has a magnetization plateau at one half of the saturation magnetization. The origin of the magnetization plateau must be the competition of the Zeeman effect and frustration [20]. Similar metamagnetic transitions were also observed in TmB_4 and TbB_4 [21–24].

In a geometrically frustrated magnetic system, a diversity of unconventional phases would be derived due to a frustrated spin interaction with lattice, orbital, and charge degrees of freedom. Thus, it was expected that perturbing the delicate equilibrium between the competing exchange interactions in a frustrated magnetic system would lead to new electronic and magnetic states. In this study, a magnetic fluctuation was induced by modifying the Shastry-Sutherland lattice in $Tb_{1-x}Y_xB_4$ and $Dy_{1-x}Y_xB_4$. The development of an anomalous weak ferromagnetism was observed at the same

*Corresponding author: chobk@gist.ac.kr

temperature as the antiferromagnetic transition. The weak ferromagnetism appeared only in the magnetic easy plane, (001) for $Tb_{1-x}Y_xB_4$, and along the magnetic easy axis, [001] for $Dy_{1-x}Y_xB_4$.

II. EXPERIMENTAL DETAILS

A stoichiometric mixture of the rare-earth metal (⩾99.9%, Alfa Aesar) and boron (99.9%, China Rare Metal Material Co., Ltd.) pieces was placed in an alumina crucible (99.8%, Samhwa Ceramic Company) with an Al (99.999%, Hydro) flux with a mass ratio of $R_{1-x}Y_xB_4$:Al = 1:50. The mixture was heated in a tube furnace with a $MoSi_2$ heating element. The heating sequence started at 300 °C to dehydrate the mixture under a high-purity argon atmosphere. After dehydration, the mixture was homogeneously melted at $T = 1600$ °C and was slowly cooled to 655 °C at a rate of 4.8 °C/h. The synthesized crystals were extracted from the Al flux using a NaOH solution. The crystal structures of the synthesized crystals were characterized using x-ray diffraction measurements (XRD; Rigaku D/MAX-2500 with a Cu target) at room temperature. The x-ray diffraction results were refined using FULLPROF software. The temperature- and magnetic-field-dependent magnetizations were performed using a superconducting quantum interference device magnetometer (SQUID; Quantum Design MPMS XL). The angle-dependent magnetic moment was measured using a SQUID with a horizontal sample rotator.

The grown single crystals were identified as single phases without any observable impurities based on the powder x-ray diffraction patterns of the pulverized single crystals, as shown in Fig. 1(a). The Y-substituted $R_{1-x}Y_xB_4$ (R = Tb and Dy) possess the tetragonal symmetry of the ThB_4-type structure and space group $P4/mbm$ (#127), similar to RB_4 [25]. The variation in the lattice parameters exhibits an almost linear decrease as the Y concentration increases, which follows Vegard's law, as illustrated in Fig. 1(b) [26]. This observation indicates that Y is well substituted in the compounds.

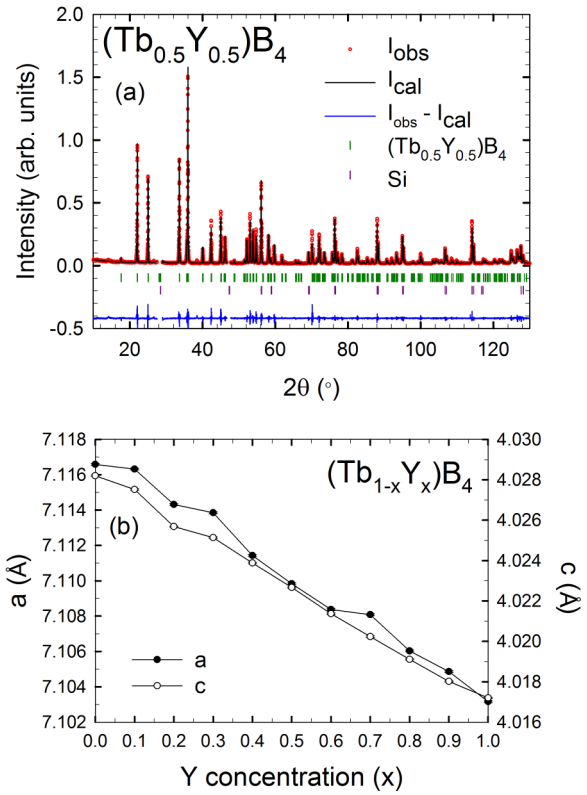

FIG. 1. (Color online) (a) Powder x-ray diffraction pattern (red) and its refinement using FULLPROF (black). (b) The variation in the a-axis and c-axis lattice parameters in terms of the Y concentration.

III. RESULT AND DISCUSSION

Figure 2(a) shows the temperature-dependent magnetization divided by the applied magnetic field ($H = 1$ T), $M(T)/H$, with the applied field parallel to the [100], [110], and [001] axes for a TbB_4 single crystal. TbB_4 was observed to have two antiferromagnetic transitions at $T_{N1} = 44$ K and $T_{N2} = 24$ K, as shown in Fig. 2(a) for $H \parallel$ to [100] and [110] [27,28]. After the first antiferromagnetic transition, the magnetic moments align in the diagonal direction in the (001) plane, and the moments are tilted approximately 23° from the diagonal direction below T_{N2} [24]. The magnetization below T_{N2} was observed to be anisotropic, even in the (001) plane. The inset of Fig. 2(a) shows the inverse magnetization, which indicates typical Curie-Weiss behavior above a Néel temperature of $T_{N1} = 44$ K. By fitting the data to the

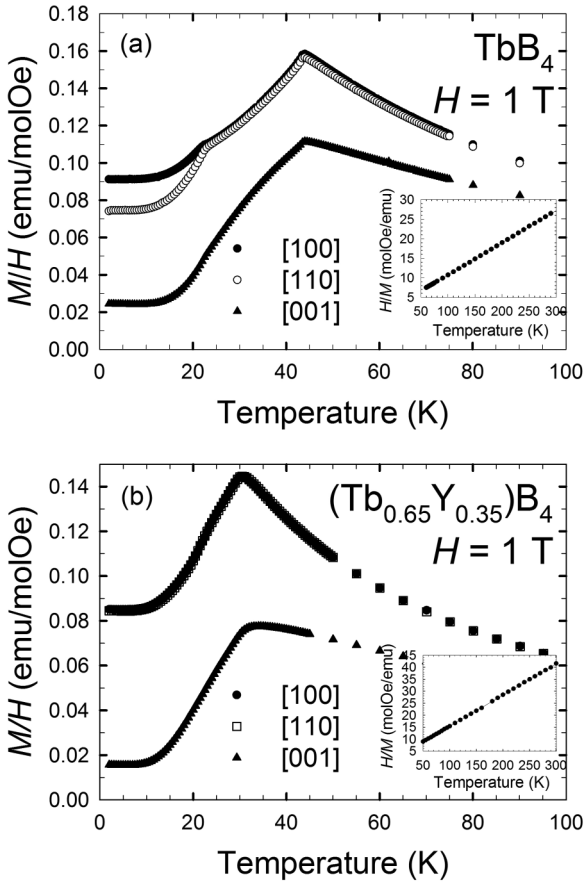

FIG. 2. Temperature-dependent magnetization divided by an applied magnetic field of $H = 1$ T, $M(T)/H$, for (a) TbB_4 and (b) $Tb_{1-x}Y_xB_4$ ($x = 0.35$) with H parallel to [100], [110], and [001]. The insets in (a) and (b) show inverse $M(T)/H$ above the antiferromagnetic transition temperatures.

Curie-Weiss equation, $\frac{M(T)}{H} = \frac{C}{(T-\theta)}$, where $C = \frac{\mu_{\text{eff}}^2}{3k_B}$, k_B is Boltzmann's constant, and μ_{eff} is the effective magnetic moment, the effective magnetic moment was observed to be equal to the theoretical value of an isolated Tb^{3+} ion ($\mu_{\text{eff}} = 9.72\mu_B$). The magnetic anisotropy, which induced the magnetic easy plane (001), was attributed to the crystalline electric field (CEF) effect acting on the $4f$ multiplet of the Tb^{3+} ion.

Figure 2(b) presents the magnetic data for a single crystal of $Tb_{1-x}Y_xB_4$ ($x = 0.35$). For the $Tb_{1-x}Y_xB_4$ ($x = 0.35$) compound, the first antiferromagnetic transition temperature decreased to $T_{N1} = 33$ K, and the second antiferromagnetic transition was not observed down to $T = 2$ K. The quadrupole interaction, which was believed to be an origin for the transition at T_{N2}, was significantly weakened by Y doping, resulting in the isotropic magnetization in the (001) plane below the antiferromagnetic transition. Curie-Weiss fitting of the inverse magnetization data [the inset of Fig. 2(b)] was performed to confirm that the concentration of Y was equal to the nominal doping ($x = 0.35$). Similar measurements and analyses were performed for the single crystals of $Tb_{1-x}Y_xB_4$ ($x = 0$, 0.1, 0.2, 0.3, 0.35, 0.4, 0.5, 0.6, 0.7, 0.8, 0.9, and 1). The Y concentrations were observed to be close to the nominal values, as shown in Fig. 3(a). The antiferromagnetic transition

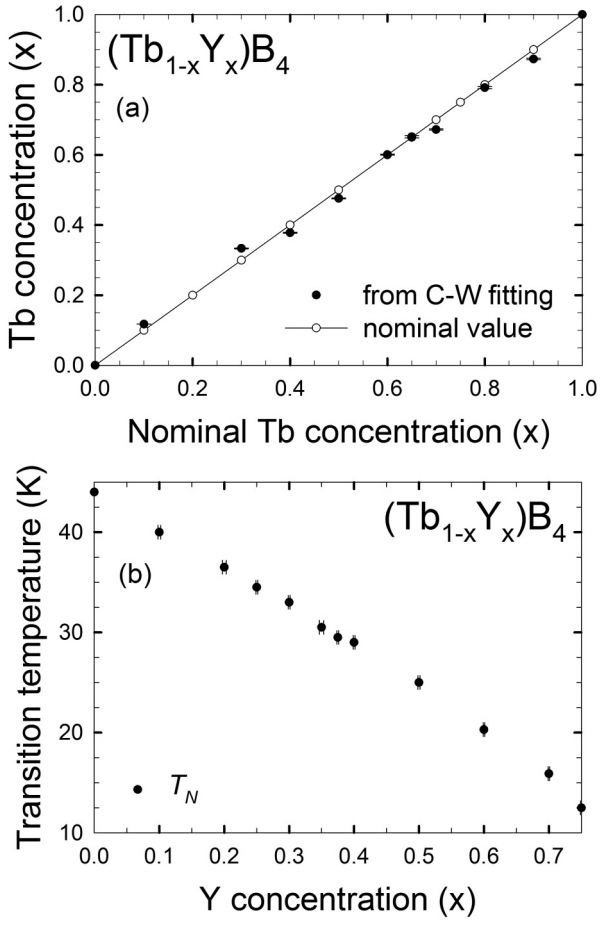

FIG. 3. (a) The Tb concentration, which is determined from Curie-Weiss fitting, vs the nominal Tb concentration in $Tb_{1-x}Y_xB_4$. (b) Variation of the Néel temperature as a function of the Y concentration.

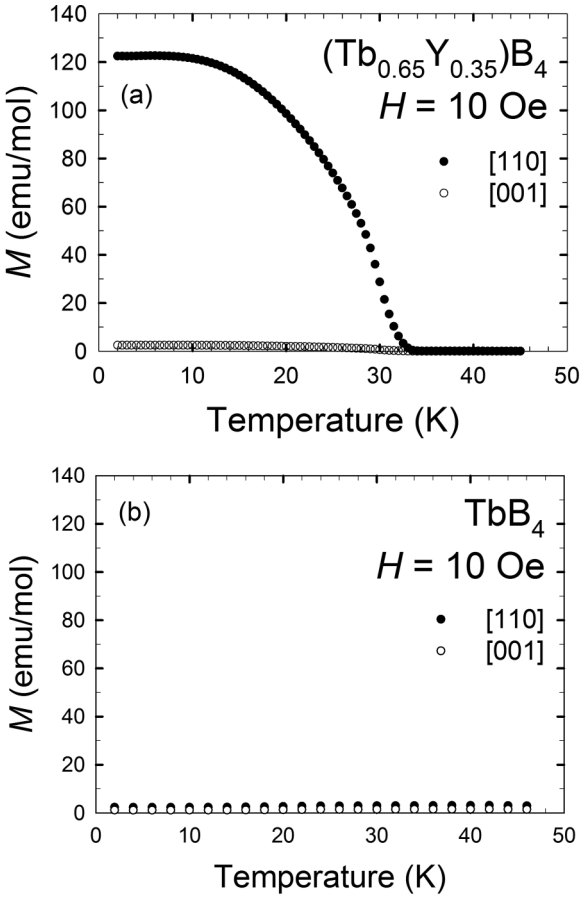

FIG. 4. Temperature-dependent magnetization $M(T)$ with an applied field of 10 Oe parallel and perpendicular to the c axis for (a) $Tb_{1-x}Y_xB_4$ ($x = 0.35$) and (b) TbB_4.

temperatures were also observed to systematically decrease as the concentration of Y increased, as shown in Fig. 3(b).

Figure 4(a) shows the temperature-dependent magnetization $M(T)$ for a single crystal of $Tb_{1-x}Y_xB_4$ ($x = 0.35$) with a small magnetic field ($H = 10$ Oe) applied parallel to [110] and [001]. The internal magnetic field in the MPMS was set to $H = 10$ Oe after the degaussing process. The measurement revealed an anomalous weak ferromagnetism along the [110] direction, whereas negligible magnetization along the [001] direction compared with the value along the [110] direction was detected, as shown in Fig. 4(a). This observation is believed to be an exotic feature because the doping element is nonmagnetic, and the magnetic impurity effect is not likely to be involved because the weak ferromagnetism is quite anisotropic. The transition temperature of the weak ferromagnetism T_C was observed to be equal to T_{N1}, which was determined when a high field ($H = 1$ T) was applied [Fig. 2(b)]. For comparison, the same measurement with $H = 10$ Oe for a single crystal of TbB_4 was performed, and the results are plotted in Fig. 4(b) with the same scale as in Fig. 4(a). The data clearly demonstrate that the weak ferromagnetism in $Tb_{1-x}Y_xB_4$ ($x = 0.35$) was induced by Y doping.

Figure 5(a) shows the temperature-dependent magnetization $M(T)$ of $Tb_{1-x}Y_xB_4$ ($x = 0.35$) with an applied field of 10 Oe in both zero-field-cooled (ZFC) and field-cooled

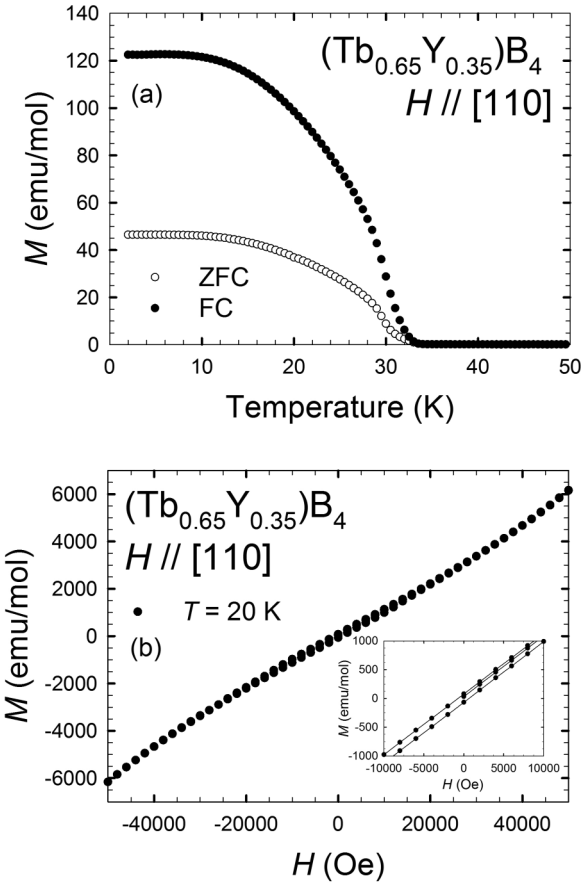

FIG. 5. (a) Temperature-dependent magnetization $M(T)$ with an applied field of 10 Oe perpendicular to the c axis for $Tb_{1-x}Y_xB_4$ ($x = 0.35$) in both zero-field-cooled (ZFC) and field-cooled (FC) modes. (b) Isothermal magnetization at $T = 20$ K for $Tb_{1-x}Y_xB_4$ ($x = 0.35$).

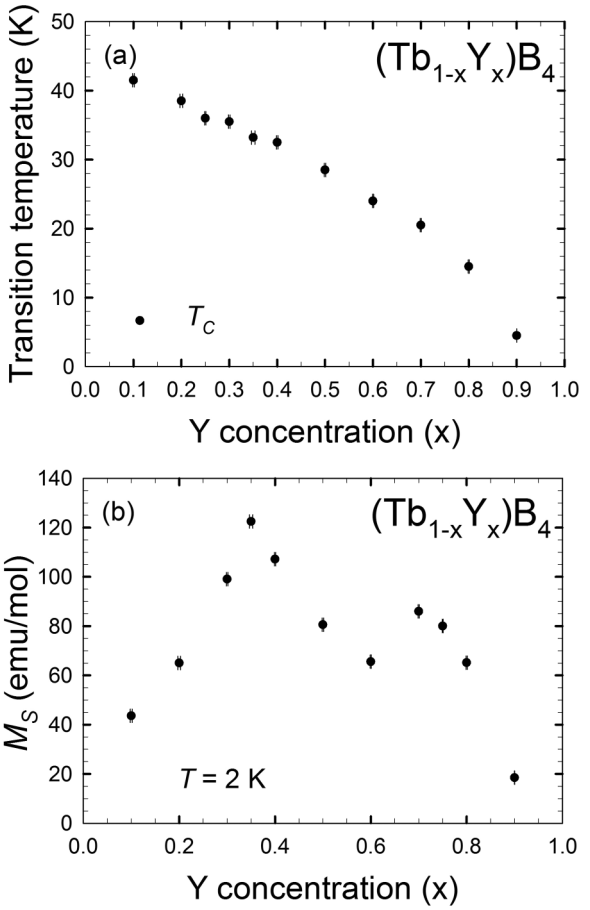

FIG. 6. (a) Variation in the Curie temperature T_C of $Tb_{1-x}Y_xB_4$ in terms of the Y concentration. (b) Variation in the spontaneous magnetization at $T = 2$ K in terms of the Y concentration.

(FC) conditions. Divergence between the ZFC and FC data was observed below the transition temperature. Isothermal magnetization at $T = 20$ K is plotted in Fig. 5(b), and the inset is an expanded plot in a field range of 10 kOe $\leqslant H \leqslant$ 10 kOe, which exhibits magnetic hysteresis near zero field. From these results, we can precisely confirm the evolution of weak ferromagnetism.

Weak ferromagnetism was also observed for the single crystals of $Tb_{1-x}Y_xB_4$ ($x = 0, 0.1, 0.2, 0.3, 0.35, 0.4, 0.5, 0.6, 0.7, 0.8, 0.9$, and 1) with the same anisotropy as $Tb_{1-x}Y_xB_4$ ($x = 0.35$) above. The variation in the weak ferromagnetic transition temperature in terms of the Y concentration was also observed to follow that of the antiferromagnetic transition, as illustrated in Fig. 6(a). This finding indicates that the weak ferromagnetic transition is closely correlated with the antiferromagnetic ordering, although the origin of the weak ferromagnetism is not yet clear. Figure 6(b) shows the saturated magnetization at $T = 2$ K in terms of the Y concentration. It was observed that the magnitude of the saturated magnetization has a strong dependence on the Y concentration and has a maximum value at $x \sim 0.35$. This finding indicates that the observed weak ferromagnetism does not have an individual atomic origin but rather is derived from an electronic and magnetic correlation effect, although the nature of the correlation is not yet clear. It can be concluded that the crystal of $Tb_{1-x}Y_xB_4$ contains the doped element, Y, in a uniform distribution on the Tb sites. As the Y concentration increased to $x = 0.35$, the doping effect began to interact, enhancing the weak ferromagnetism. Further doping above $x = 0.35$ was observed to weaken the interaction, reducing the weak ferromagnetism.

To investigate magnetic anisotropy within the (001) plane, the angular dependence of the weak ferromagnetism was measured. A single crystal, $Tb_{1-x}Y_xB_4$ ($x = 0.35$), was cooled below the transition temperature with a weak field of 10 Oe applied along the [110] direction. Then, the magnetization was measured while the sample was rotating, as plotted in Fig. 7(a). The angular dependence of the moment along the [110] direction indicates that the weak ferromagnetism can be established in a specific direction, i.e., the [110] direction in Fig. 7(c), by applying a magnetic field along the direction above the transition temperature. Figure 7(b) shows the saturated magnetic moment of the weak ferromagnetism along each specific direction within the (001) plane at $T = 2$ K. It is clear that the magnitude of the weak ferromagnetism has a local maximum along the principal axis and a local minimum along the diagonal axis within the (001) plane. Because the magnetic structure of TbB_4 was characterized by orthogonal dimers, the weak ferromagnetism was observed to be smaller

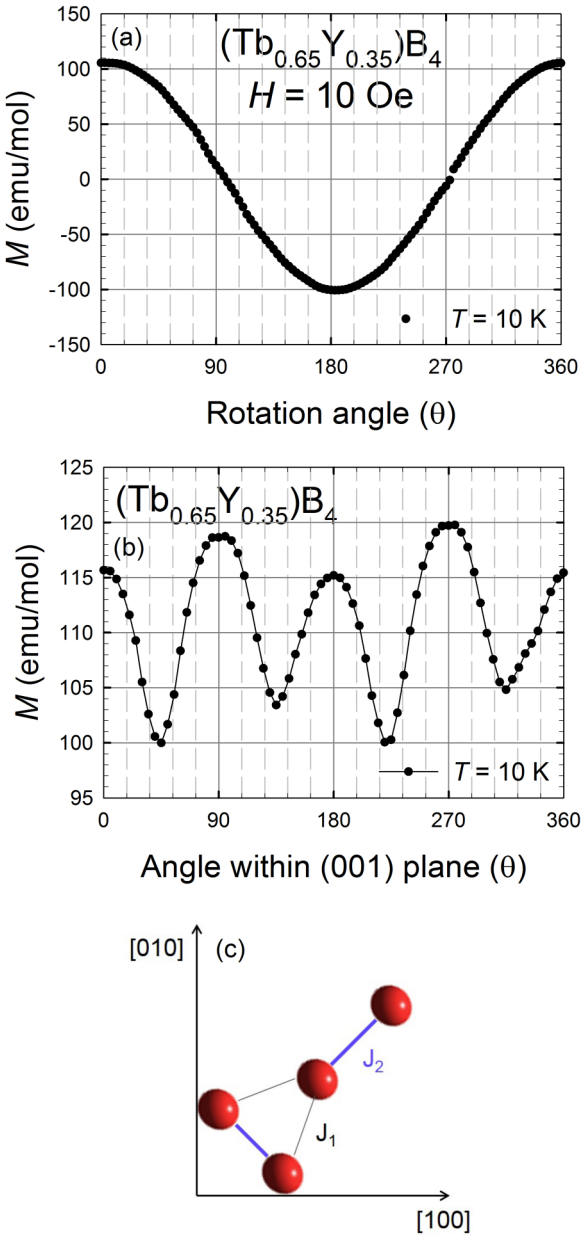

FIG. 7. (Color online) (a) Spontaneous magnetization along [110] at $T = 2$ K in terms of the rotation angle of the sample. (b) Spontaneous magnetization at $T = 2$ K along the specific directions within the (001) plane, i.e., along the x axis for $\theta = 0°$, [110] for $\theta = 45°$, and the y axis for $\theta = 90°$. (c) Representation of Tb dimers within the (001) plane with exchange interaction strengths J_1 and J_2.

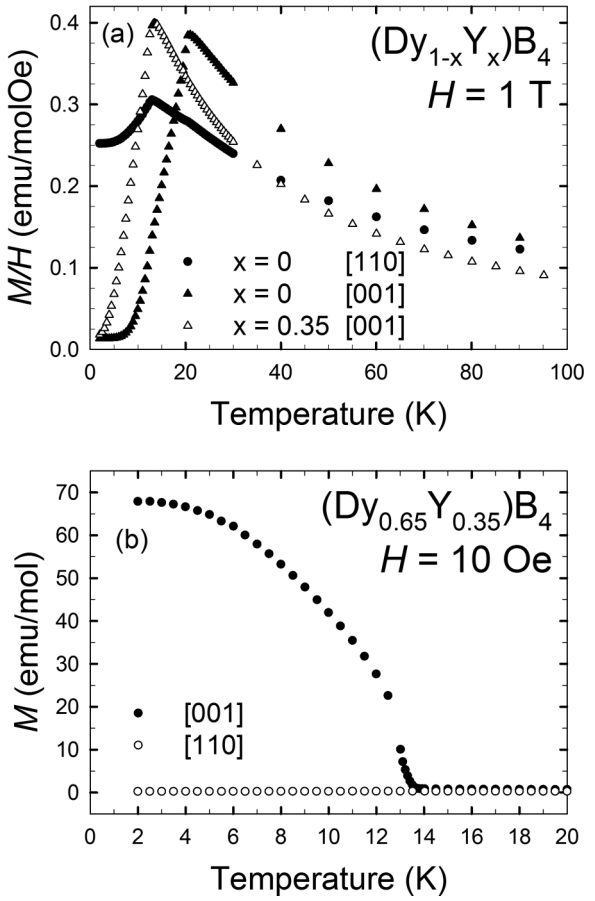

FIG. 8. (a) Temperature-dependent magnetization divided by an applied magnetic field of $H = 1$ T, $M(T)/H$ for DyB_4 with H parallel to [110] and [001] and for $Dy_{1-x}Y_xB_4$ ($x = 0.35$) with H parallel to [001]. (b) Temperature-dependent magnetization $M(T)$ with an applied field of 10 Oe parallel and perpendicular to the c axis for $Dy_{1-x}Y_xB_4$ ($x = 0.35$).

along the dimer than along the direction at 45° from the dimer, as shown in Fig. 7(c).

Figure 8(a) shows the temperature-dependent magnetization divided by the applied field ($H = 1$ T) along the [001] direction, $M(T)/H$, for single crystals of DyB_4 and $Dy_{1-x}Y_xB_4$ ($x = 0.35$). DyB_4 was observed to be a geometrically quadrupolar frustrated system and exhibited an antiferromagnetic transition at $T_{N1} = 20$ K with collinear ordering along the [001] direction and a second transition at $T_{N2} = 13$ K due to the quadrupolar interaction [18,29,30]. The corresponding transitions were demonstrated in $M(T)$ data for DyB_4 [Fig. 8(a)] at $T_{N1} = 20$ K and $T_{N2} = 13$ K. The transition at $T_{N1} = 20$ K was observed to decrease to $T_{N1} = 14$ K with 35% Y doping, as shown in Fig. 8(a). Figure 8(b) shows the magnetizations with an applied field of $H = 10$ Oe along the [110] and [001] directions. It was clearly observed that a weak ferromagnetic transition was established at $T_{N1} = 14$ K in the [001] direction, in which antiferromagnetic collinear ordering occurred. The weak ferromagnetism was not observed in the [110] direction for a single crystal of $Dy_{1-x}Y_xB_4$ ($x = 0.35$).

From the magnetization data under a low field of $H = 10$ Oe for $Tb_{1-x}Y_xB_4$ ($x = 0.35$) and $Dy_{1-x}Y_xB_4$ ($x = 0.35$), anomalous weak ferromagnetism was observed to be induced by Y doping for both compounds. In addition, the weak ferromagnetic moment was also observed to be established within the (001) plane for $Tb_{1-x}Y_xB_4$ ($x = 0.35$) and along the [001] direction for $Dy_{1-x}Y_xB_4$ ($x = 0.35$), where antiferromagnetic ordering occurred for both compounds. It appears that the occurrence of the weak ferromagnetism as a result of Y doping is a common feature for tetraboride compounds, RB_4, which indicates that the weak ferromagnetism would be closely correlated with a frustrated magnetic system with orthogonal dimers in a Shastry-Sutherland lattice.

One of the possible scenarios for the occurrence of the weak ferromagnetism might be the canting of Tb moments due to Y doping at the Tb sites. The canting model can qualitatively explain the anisotropy of the weak ferromagnetism in the (001) plane, as shown in Fig. 7(b). The magnetic moment along the principal axis should be $\sqrt{2}$ times larger than that along the diagonal axis. However, the ratio between the maximum and minimum moments is considerably smaller than the expected value. In addition, the canting model cannot be applied for the $Dy_{1-x}Y_xB_4$ system because the weak ferromagnetism occurred along the direction in which antiferromagnetic collinear ordering occurred.

Notably, a first-order transition to a ferromagnetic state was observed in PrB_4 [31]. The magnetism in PrB_4 was induced by the coupling of singlets, which were lifted from the degeneracy of the Hund's rule ground-state multiplet of the Pr ion. Although the mechanism of weak ferromagnetism for $R_{1-x}Y_xB_4$ (R = Tb and Dy) in this paper is not fully understood, the weak ferromagnetism in the $R_{1-x}Y_xB_4$ (R = Tb and Dy) system is not believed to have an origin in the CEF effect for lifting the degeneracy of the Hund's rule ground-state multiplet of the Tb and Dy ions. The occurrence of weak ferromagnetism and its dependence on the Y concentration are similar for the two systems of $R_{1-x}Y_xB_4$ (R = Tb and Dy), even though the two systems have quite different anisotropies.

The ground state of RB_4 consists of singlet dimers in a Shastry-Sutherland lattice, as determined from neutron diffraction experiments. The magnetic moments of a dimer point along $\sim 23^\circ$ from the (110) direction in the (001) plane for TbB_4 and along the c axis for DyB_4. Now, consider Y substitution of the R elements. As the nonmagnetic Y replaces magnetic R elements, the effective antiferromagnetic exchange interactions are reduced to $J_1\langle n\rangle$ and $J_2\langle n\rangle$, where $\langle n\rangle$ is the concentration of the R element, and the Néel temperature should decrease, as demonstrated in Fig. 3(b). In addition, spinless singlets are broken by the Y substitution and converted into nonzero moments. The observed weak ferromagnetism is likely due to the ferromagnetic interaction of the generated moments, which suggests that their environments are the same. This explanation is consistent with the observations that the ferromagnetic moments are in the (001) plane and along the c axis for $Tb_{1-x}Y_xB_4$ and $Dy_{1-x}Y_xB_4$, respectively, and that $T_C = T_N$. The pointing angle of the generated moment is determined by the competition between the crystalline anisotropy favoring the dimer direction and the ferroquadrupolar interaction favoring the direction perpendicular to the local dimer direction. It appears that an appropriate selection of the interaction parameters can generate the angular dependence of the weak ferromagnetic moment in Fig. 7(b). In addition, as observed in Fig. 6(b), the generation rate of the ferromagnetic moment M_s by the Y substitution is $\sim$400 emu/(mol$x$), with x being the Y concentration, in the small x and symmetrically small $1-x$ limits. The magnetic moment of Tb is $\sim 9.5\mu_B = 8.8\times 10^{-20}$ emu; thus, if all Y substitutions generate the full Tb moments, the generation rate must be $\sim 5.3\times 10^4$ emu/(mol$x$). The measured rate in Fig. 6(b) is smaller than this value by a factor of $\sim 10^2$, which is not inconsistent with the expectation from the picture presented above by the Boltzmann factor of $\exp(\frac{-J_1}{T})$. This factor originates from the observation that Y substitution of both Tb atoms on a dimer has a lower energy by J_1 than the separate substitution of two dimers. As the Y concentration further increases, the ratio of Y-Y dimers to Y-Tb increases such that the induced moment is expected to reach a maximum before $x = 0.5$, as was indeed observed.

IV. CONCLUSION

This work showed the experimental discovery of the development of weak ferromagnetism induced by nonmagnetic ion substitution in the geometrically frustrated system of $R_{1-x}Y_xB_4$ (R = Tb and Dy). The exotic weak ferromagnetism occurred only along the magnetic easy plane, i.e., the (001) plane for $Tb_{1-x}Y_xB_4$, and along the magnetic easy axis, i.e., the [001] axis for $Dy_{1-x}Y_xB_4$. In addition, the weak ferromagnetism in $Tb_{1-x}Y_xB_4$ was observed to be anisotropic, even within the (001) plane; that is, there was a local minimum along the Tb dimer and a local maximum away from the dimer by 45°. We believe that the occurrence of the weak ferromagnetism is closely related to the frustration of magnetic dimers in the Shastry-Sutherland lattice because the magnitude of the weak ferromagnetism has a strong dependence on the Y concentration, indicating the collective correlation effects of the doping. The Tb moment generated by Y substitution was expected to align ferromagnetically because of the competition between the crystalline anisotropy and the ferroquadrupolar interaction. The unusual weak ferromagnetism is not yet fully understood, and an appropriate theoretical mechanism should be investigated.

ACKNOWLEDGMENTS

B.Y.K. would like to thank S. S. Lee for helpful discussions and M. S. Song for experimental assistance. This work was supported by National Research Foundation of Korea (NRF) grants funded by the Korean government (MSIP; Grants No. 2011-0028736 and No. 2013K000315).

[1] M. J. Harris, S. T. Bramwell, D. F. McMorrow, T. Zeiske, and K. W. Godfrey, Phys. Rev. Lett. **79**, 2554 (1997).
[2] J. S. Gardner, S. R. Dunsiger, B. D. Gaulin, M. J. P. Gingras, J. E. Greedan, R. F. Kiefl, M. D. Lumsden, W. A. MacFarlane, N. P. Raju, J. E. Sonier, I. Swainson, and Z. Tun, Phys. Rev. Lett. **82**, 1012 (1999).
[3] S. T. Bramwell and M. J. P. Gingras, Science **294**, 1495 (2001).
[4] S.-H. Lee, C. Broholm, W. Ratcliff, G. Gasparovic, Q. Huang, T. H. Kim, and S.-W. Cheong, Nature (London) **418**, 856 (2002).
[5] H. Kageyama, K. Yoshimura, R. Stern, N. V. Mushnikov, K. Onizuka, M. Kato, K. Kosuge, C. P. Slichter, T. Goto, and Y. Ueda, Phys. Rev. Lett. **82**, 3168 (1999).
[6] B. S. Shastry and B. Sutherland, Physica **108B**, 1069 (1981).
[7] S. Miyahara and K. Ueda, Phys. Rev. Lett. **82**, 3701 (1999).

[8] A. Läuchli and D. Poilblanc, Phys. Rev. Lett. **92**, 236404 (2004).
[9] E. Bose, S. Karmakar, and B. K. Chaudhuri, J. Phys. Condens. Matter **19**, 486201 (2007).
[10] J. G. S. Duque, E. Miranda, A. M. O. Belon, L. Bufaiçal, C. Rettori, and P. G. Pagliuso, Physica B (Amsterdam, Neth.) **398**, 430 (2007).
[11] H. D. Zhou, J. Lu, R. Vasic, B. W. Vogt, J. A. Janik, J. S. Brooks, and C. R. Wiebe, Phys. Rev. B **75**, 132406 (2007).
[12] S. Seki, Y. Yamasaki, Y. Shiomi, S. Iguchi, Y. Onose, and Y. Tokura, Phys. Rev. B **75**, 100403(R) (2007).
[13] A. Koga and N. Kawakami, Phys. Rev. Lett. **84**, 4461 (2000).
[14] J. Liu, N. Trivedi, Y. Lee, B. N. Harmon, and J. Schmalian, Phys. Rev. Lett. **99**, 227003 (2007).
[15] C. H. Chung and Y. B. Kim, Phys. Rev. Lett. **93**, 207004 (2004).
[16] J. Etourneau, J. P. Mercurio, A. Berrada, and P. Hagenmuller, J. Less Common Met. **67**, 531 (1979).
[17] K. H. J. Buschow and J. H. N. Creyghton, J. Chem. Phys. **57**, 3910 (1972).
[18] S. Ji, C. Song, J. Koo, J. Park, Y. J. Park, K. B. Lee, S. Lee, J. G. Park, J. Y. Kim, B. K. Cho, K. P. Hong, C. H. Lee, and F. Iga, Phys. Rev. Lett. **99**, 076401 (2007).
[19] R. Watanuki, T. Kobayashi, R. Noguchi, and K. Suzuki, J. Phys. Conf. Ser. **150**, 042229 (2009).
[20] S. Michimura, A. Shigekawa, F. Iga, M. Sera, T. Takabatake, K. Ohoyama, and Y. Okabe, Physica B (Amsterdam, Neth.) **378–380**, 596 (2006).
[21] F. Iga, A. Shigekawa, Y. Hasegawa, S. Michimura, T. Takabatake, S. Yoshii, T. Yamamoto, M. Hagiwara, and K. Kindo, J. Magn. Magn. Mater. **310**, e443 (2007).
[22] K. Siemensmeyer, E. Wulf, H.-J. Mikeska, K. Flachbart, S. Gabáni, S. Matas, P. Priputen, A. Efdokimova, and N. Shitsevalova, Phys. Rev. Lett. **101**, 177201 (2008).
[23] S. Yoshii, T. Yamamoto, M. Hagiwara, T. Takeuchi, A. Shigekawa, S. Michimura, F. Iga, T. Takabatake, and K. Kindo, J. Magn. Magn. Mater. **310**, 1282 (2007).
[24] S. Yoshii, K. Ohoyama, K. Kurosawa, H. Nojiri, M. Matsuda, P. Frings, F. Duc, B. Vignolle, G. L. J. A. Rikken, L. P. Regnault, S. Michimura, and F. Iga, Phys. Rev. Lett. **103**, 077203 (2009).
[25] J. Etourneau and P. Hagenmuller, Philos. Mag. B **52**, 589 (1985).
[26] A. R. Denton and N. W. Ashcroft, Phys. Rev. A **43**, 3161 (1991).
[27] F. Elf, W. Schafer, and G. Will, Solid State Commun. **40**, 579 (1981).
[28] J. C. Gianduzzo, R. Georges, B. Chevalier, J. Etourneau, P. Hagenmuller, G. Will, and W. Schafer, J. Less Common Met. **82**, 29 (1981).
[29] R. Watanuki, G. Sato, K. Suzuki, M. Ishihara, T. Yanagisawa, Y. Nemoto, and T. Goto, J. Phys. Soc. Jpn. **74**, 2169 (2005).
[30] R. Watanuki, H. Mitamura, T. Sakakibara, G. Sato, and K. Suzuki, Physica B (Amsterdam, Neth.) **378**, 594 (2006).
[31] G. A. Wigger, E. Felder, R. Monnier, H. R. Ott, L. Pham, and Z. Fisk, Phys. Rev. B **72**, 014419 (2005).